DOI: 10.48011/asba.v2i1.1635

Electronic Instrumentation for Shape Memory Alloy Actuators

Luzia Marcela Magalhães Lopes *. Maxsuel Ferreira Cunha. José Marques Basílio Sobrinho*** Cícero da Rocha Souto ****. Andreas Ries*****. Jordashe Ivys Souza Bezerra******. Euler Cássio Tavares de Macêdo*********

**Electrical Engineering Department, Federal University of Paraiba - UFPB, João Pessoa, PB, Brazil (e-mail: luzia.lopes@cear.ufpb.br)*
***Electrical Engineering postgraduate Program, Federal University of Campina Grande - UFCG, Campina Grande, PB, Brazil (e-mail: maxsuel.cunha@ee.ufcg.edu.br)*
****Mechanical Engineering postgraduate Program, São Carlos School of Engineering- EESC-USP, São Carlos, SP, Brazil (e-mail: josemarquesbasilio@gmail.com)*
****** Electrical Engineering Department, Federal University of Paraiba - UFPB, João Pessoa, PB, Brazil (e-mail: cicerosouto@cear.ufpb.br)*
****** Electrical Engineering Department, Federal University of Paraiba - UFPB, João Pessoa, PB, Brazil (e-mail: ries750@yahoo.com.br)*
*******Electrical Engineering Department, Federal University of Paraiba - UFPB, João Pessoa, PB, Brazil (e-mail: jordashe.bezerra@cear.ufpb.br)*
********Electrical Engineering Department, Federal University of Paraiba - UFPB, João Pessoa, PB, Brazil (e-mail: euler@cear.ufpb.br)*

Abstract: Shape memory alloy (SMA) actuators have been increasingly found applications due to their low weight and high power capacity. Additionally they are able to function as a sensor. Upon phase transformation, the material changes its electrical resistance. Phase transformation in SMAs occurs either by loading or heating the material. Since SMAs materials are usually metals, heat can be produced by passing an electric current through the alloy. This idea in mind, the present work reports the development of electronic circuits for power supply, current measurement and voltage measurement for shape memory alloy actuators. For validation of the operation of the designed circuits, a NiTi helical spring type alloy actuator was tested. The actuator was mounted on a mechanical platform; it was possible to determine its thermal behavior and force generation. Characteristic operation curves of the helical spring type actuator are presented.

Resumo: Os atuadores de liga com memória de forma (LMA) têm sido cada vez mais encontrados devido ao seu baixo peso e alta capacidade de energia. Além disso, eles são capazes de funcionar como um sensor. Após a transformação de fase, o material altera sua resistência elétrica. A transformação de fase nas LMAs ocorre carregando ou aquecendo o material. Como os materiais das LMAs são geralmente metais, o calor pode ser produzido passando uma corrente elétrica através da liga. Com esta idéia, o presente trabalho relata o desenvolvimento de circuitos eletrônicos para alimentação, medição de corrente e medição de tensão para atuadores de liga com memória de forma. Para validação da operação dos circuitos projetados, um atuador de liga de mola helicoidal do tipo NiTi foi testado. O atuador foi montado em uma plataforma mecânica; foi possível determinar seu comportamento térmico e geração de força. São apresentadas curvas de operação características do atuador do tipo helicoidal de mola.

Keywords: Thermal actuator; Material with shape memory; Current source.

Palavras-chaves: Atuador térmico; Material com memória de forma; Fonte de corrente.

1. INTRODUCTION

Shape Memory Alloys (SMAs) are functional materials with various industrial applications, including the medical field of human rehabilitation. It has been shown (Silva, 2013) that a 3 degree of freedom robotic finger structure using shape memory alloy actuators can be driven by an electric current. The finger was constructed with SMA actuators using a NiTi 1:1 stoichiometry wire of 0.31 mm diameter. For that task a voltage-controlled continuous current amplifier with bipolar transistors and maximum current of 2 A was developed. The maximum current for robotic finger activation was 900 mA, heating the wire up to 130°C.

The displacement of a SMA helical spring type actuator can be estimated through its coil inductance (Kim, 2012). The inductance of the coil was determined measuring the voltage and the transient electric current response. A current amplifier circuit was used to power the SMA coil

using a 8 V wave with modulated pulse width (PWM). Current measurement was achieved using an oscilloscope with current probe. The diameter of the SMA helical spring was 6 mm and the wire diameter was 0.508 mm, with a total length of 50 mm. The measurements were performed for displacements between 0.50 and 150 mm.

Hau et al. (Hau, 2017) presented a robot for ankle rehabilitation that utilizes a shape memory alloy (SMA) actuator to provide flexion and plantar dorsiflexion in the foot during rehabilitation exercises. The SMA wire actuator was activated by Joule heating so that it can reach the temperature initiating austenite formation. For the actuation of the SMA actuator, a 10 V DC voltage source supporting 30 A output current was available. Force and displacement sensors were also used.

Hwang et al. (Hwang, 2017) discussed the conceptual design, the operating principle, the parametric analysis, the experimental characterization of the conduction and the verification of the operational performance of a rotary actuator using shape memory alloy wires. In their prototype, SMA wires were electrically heated by the application of electric current that is, heating by Joule and cooled by means of natural convection. A three-phase pulsed voltage source with power amplifier was used. The fundamental characterization of the conduction was carried out to investigate the influence of pulse width modulated voltage sources on the performance of the actuators for the condition of fixed amplitude and excitation frequency.

The literature reports research (Basílio Sobrinho, 2017) dealing with the electronic instrumentation for the characterization of a thermoelectric motor using SMA mini-springs as an active element of the actuator. In this work, besides designing the thermoelectric motor, power circuits were developed to activate each SMA actuator. Control software and pulse width modulation were used for activating the actuators (Basílio Sobrinho, 2017).

Researchers have deposited a SMA Cu-Al-Ni alloy on polyimide strip with bidirectional displacement (Akash, 2017). The electronic instrumentation for driving the device and measuring the behavior of the alloy was composed of a programmable voltage source, K-type thermocouples, and a 22-channel data acquisition system. The heating and cooling cycles were recorded by a laser displacement sensor. Three different voltages, 2 V, 2.5 V and 3 V with frequencies of 0.05 Hz and 0.5 Hz were used for analysis. The absence of fatigue was tested for 500 cycles.

The contribution of this work to the literature is the presentation of a simple and cheap electronic instrumentation for driving shape memory alloy actuators and making all the measurements required for characterization; this means the material characterization and the actuator control in different applications.

2. EXPERIMENTAL PROCEDURE

The experimental procedure for the development of this research was divided in several parts. The first one consisted in the elaboration of the constant current source circuits, current measurement circuit, voltage measurement circuit and signal conditioning of the load cell. In this procedure, temperature signals were also collected directly on a data acquisition board connected to the K-type thermocouple.

The second part of the work was to develop a mechanical structure for characterization of a NiTi spring type actuator. Finally, a software interface produced the current control signal and recorded the current, voltage, force and temperature measurements of the SMA actuator. Initially all circuits were simulated with commercial software and then mounted on circuit boards.

The main circuit for driving a SMA actuator by Joule effect is a current source or a variable voltage source. The source is intended to provide the heating current so that the actuator can change shape and produce force. In the case of NiTi SMA, this shape change is accompanied by a transformation of the martensite phase to the austenite phase.

In this work, it was opted to design a current source using the IRF740 MOSFET transistor and an LM324 operational amplifier with negative feedback. This circuit has as input a control signal which may be for example a PWM signal; in this case the output of the circuit accompanies the input signal. The maximum current of this circuit is limited to approximately 1.5 A.

The terminal of the source was attached to a current measuring circuit, which was connected in series with the SMA actuator; the voltage measuring circuit was connected to the actuator. Current and voltage are required for determining the variation of the electrical resistance of the actuator and also for use with control variables when necessary. In Fig. 1 the circuit diagram of the developed circuit is shown, highlighting the connection of the load, which is the SMA actuator in this application.

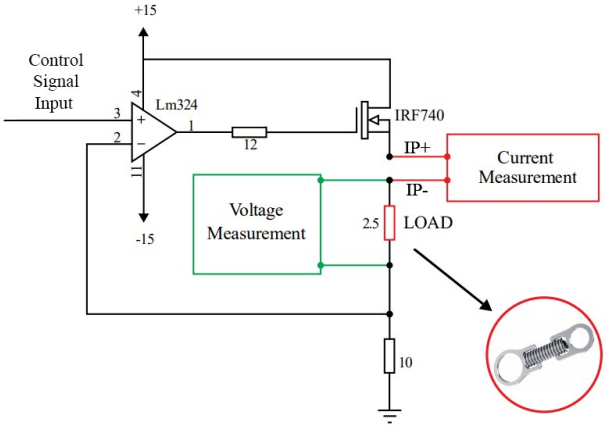

Fig. 1: Schematic of the current source circuit

In the circuit of Fig. 2, an operational amplifier configured as a subtractor is connected across the load to measure the voltage drop on it. The output signal (output 1) is connected to an input of the data acquisition system, to read out that voltage.

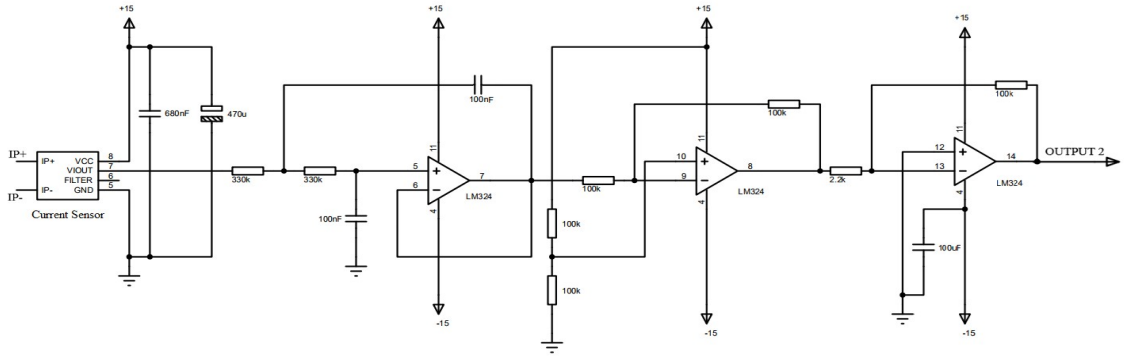

Fig. 3. Circuit for current measurement

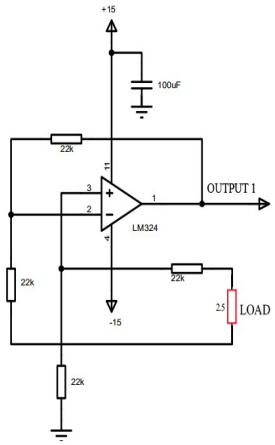

Fig. 2: Circuit for voltage measuring

In Fig. 3 the electrical circuit diagram for measuring electric current passing through the SMA actuator is shown. This circuit has as main component the ACS712 integrated circuit which is a hall effect-based linear current sensor with 2.1 kV RMS voltage isolation and low resistance current conductor. This current sensor has sensitivity between 66 and 185 mV/A. This means, in this case, amplification was necessary.

The sensor conditioner circuit was composed of a second order active filter with a cutoff frequency of about 5.0 Hz. This filter was necessary for eliminating high frequency noise since this work focuses at the low frequency switching.

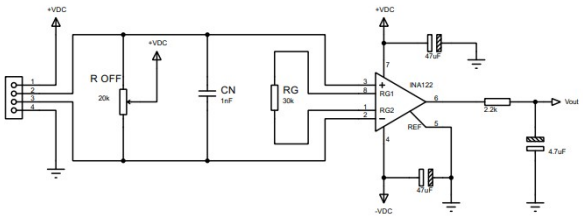

Fig 4: Charge cell signal conditioning circuit

Then an amplifier in inverter configuration with gain equal to 1 was used to eliminate the offset. Finally another amplifier was able to restore the original phase of the input signal, with gain of approximately 45.

For the signal conditioning of the load cell providing the force measurement, a circuit was developed shown in Fig. 4, using the INA122 instrumentation amplifier. A gain of 45 was calculated based on the gain equation provided by the component datasheet. This gain was sufficient for the 350 Ohm load cell signal to be distinguished from noise.

The load used in the circuits was a NiTi helical spring type actuator with resistance of 2.5 Ohm, 12 mm center distance of the terminals and a useful contracted length (state of rest) of 7.5 mm. The spring had 27 active turns, 0.22 mm wire diameter and 1.27 mm spring diameter. Its total elongation can reach up to 600% of its original size.

This actuator, at rest, has an austenite crystalline structure with mechanical behavior similar to a mechanical spring. When stretched by the imposition of a mechanical force, a part of the austenite transforms into martensite, which does not happen in common mechanical springs. When elongated and heated, it tends to return to its original form, generating mechanical force if the structure is fixed.

The spring-type actuator used in this research to validate the designed circuits via actuator property characterization is highlighted in Fig. 1.

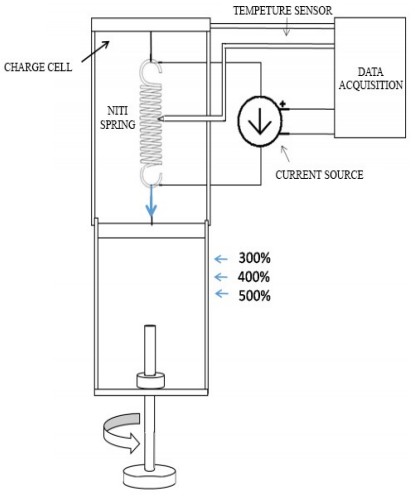

Fig.5: Structure for collecting experimental results.

For the collection of experimental results of the NiTi spring type actuator it was necessary to construct a mechanical structure. In Fig. 5 a schematic of the system used for the characterization of the actuator is shown. The actuator has been attached to the upper part of the load cell

(fixed) and the lower (movable) part of the structure. The instrumentation developed and the data acquisition system were connected at the terminals of the actuator.

The lower part of the structure was moved by the action of a spindle extending the actuator to 300, 400 and 500% of its original size. The choice of the 300 to 500% range was made, based on the scientific literature surrounding NiTi actuators. In this range, the actuator has greater efficiency with respect to force, below 300% there is no significant gain.

For each elongation step, a current pulse passed through the actuator and the temperature and force parameters were measured. These current pulses had different durations: 5, 10 and 15 s. These heating times were used to test the stabilization of the actuator, that is, they served to identify which pulse width was sufficient for the actuator to enter permanent regime.

3. RESULTS AND DISCUSSION

Initially, a 400 mA and 5 s current pulse was applied to the SMA actuator. The chosen amplitude of the electric current was based on the austenite formation temperature of the spring. This value was tested previously to identify which current would produce the greatest displacement of the spring. In this case, with the current rise above 400 mA, the actuator would not do more displacement work but would only dissipate power. Fig. 6 shows the current and temperature pulse curves as a function of time. For each elongation value, a current pulse was applied. However, since the pulses were the same, they overlap in the graph.

The thermal behavior showed that for 500% elongation the actuator reached a lower heating temperature for the pulse width of 5s. For the 400 and 300% elongations the temperature increased accordingly. This behavior can be explained taking into account that the more elongated the actuator is, the more effective is the heat exchange with the environment, allowing a better thermal dissipation and lower final temperature.

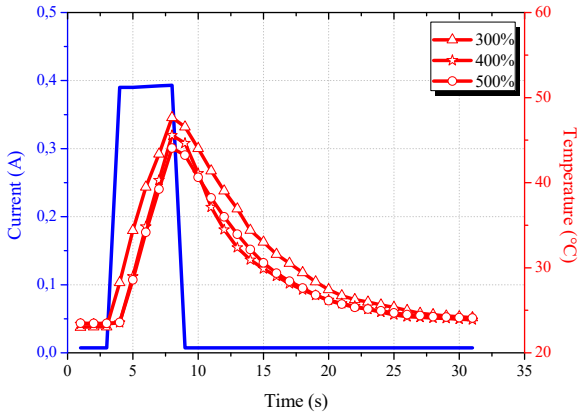

Fig .6: Temperature response (5 s current pulse)

In Fig. 7 the actuator temperature response to a 400 mA / 10 s pulse is presented. The temperature grows with reduced elongation, similar to previously presented results. However, in this situation, the actuator has reached higher temperatures. While 5 s pulses heated the actuator to temperatures between 40 and 50°C, 10 s pulses lead to temperatures between 55 and 70°C. This behavior was expected because the larger the pulse width, the greater the amount of heat accumulated by the actuator. Regarding heat dissipation, both cases show that the actuators return to the initial ambient temperatures within 25-30 s.

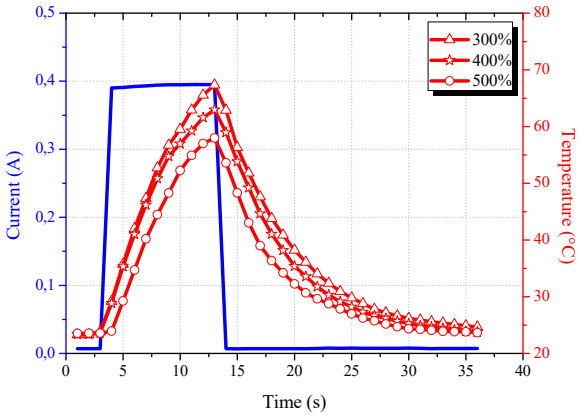

Fig.7: Temperature response (10 s current pulse)

Fig. 8 shows that with increasing elongation the actuator dissipates less energy equal to the previous cases. The high temperature level was between 60 and 75°C. However, something different occurred for elongations below 400%; here, a beginning of a temperature stabilization near 13 s becomes visible. This phenomenon may be related to the finalization of the austenite phase formation at this specific actuator condition.

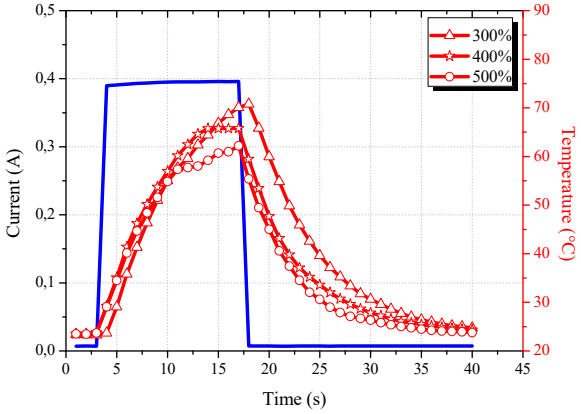

Fig.8: Temperature response (15 s current pulse)

Simultaneously with the application of current pulse and temperature data collection, the force that the SMA actuator exerts on the structure was recorded. This information is very relevant for practical applications of these actuators; it demonstrates the minimum and maximum force the actuator is able to produce.

Fig. 9 shows the force response of the actuator for the condition of a 400 mA pulse current with 5 s duration. In this graph it can be observed that the elongation imposed on the actuator determines an initial force, that is, the actuator does not exert a zero rest force; additionally the value of the initial force increases with increase in elongation. Another fact is that with increasing actuator heating, the force also increases reaching the maximum limit for the corresponding heat. Numerical values of relative maximum forces were 1.03, 1.09 and 1.23 N approximately, for strains of 300, 400 and 500% respectively.

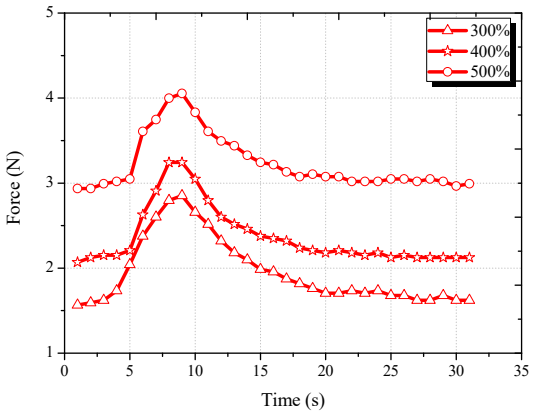

Fig.9: Force response for a 5 second current pulse

Fig. 10 displays the force response of the actuator for a 400 mA current pulse with 10 s duration. The force response is very similar to the previous case with respect to the initial force. The force increase with rising temperature of the actuator. However, the relative maximum forces were higher reaching 1.63, 1.67 and 1.70 N for 300, 400 and 500% strain respectively. This fact was expected because the 10 s pulse heated the actuator much more up the 5 s current pulse.

In Fig. 11 the force response of the actuator is shown for a 400 mA / 15 s current pulse. The arguments of the previous discussion apply to this situation. However, the relative maximum forces were different, reaching 1.57, 1.70 and 1.95 N for the 300, 400 and 500% strains, respectively.

There was a small difference in the 300% strain situation. Here the force decreased somewhat, but, this fact can be attributed to a complete austenite formation during the 15 s. It did not occur in the other experiments because there will be much more martensite to be transformed into austenite. The force curve for the 400% strain condition showed a better stabilization than in other situations.

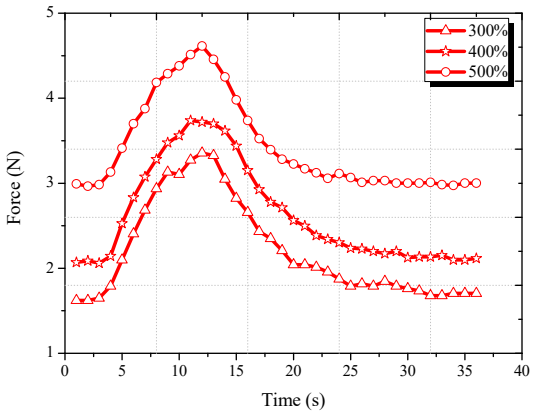

Fig.10: Force response for a 10 second current pulse

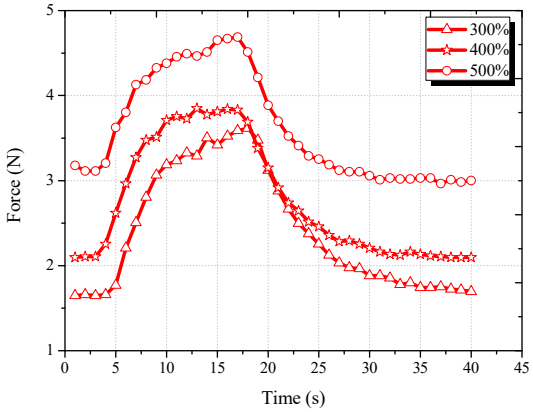

Fig. 11: Force response for a 15 second current pulse

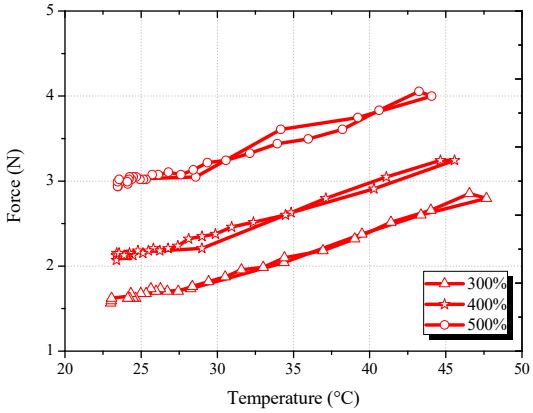

Fig. 12: Hysteresis response (5 s current pulse)

From the collected temperature and force results it was possible to visualize the characteristic hysteresis behavior of shape memory alloys. From Fig. 12 can be seen that greater heat loss occurs for the 500% strain condition. In this case, the current pulse was smaller, but the amount of martensite formed was higher and this causes the actuator to

return via another path during cooling since the austenite formation time is path dependent.

Fig. 13 and Fig. 14 show different hysteresis evolutions, but always presenting a growth with the increase in the actuator's operating time. This was expected because the curve grows completely. A fact to be highlighted is that in the condition of a 400% strain, the hysteresis curves were much narrower, indicating lower loss (for all three operating times).

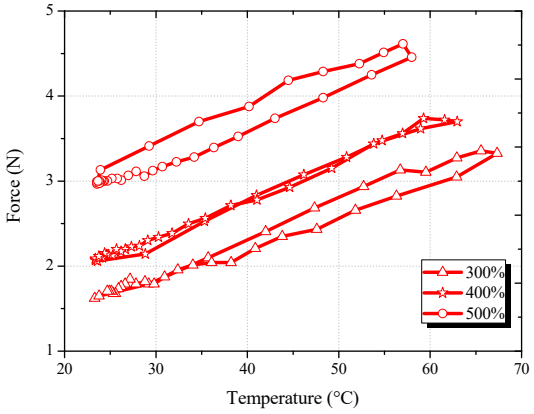

Fig. 13: Hysteresis curves (10 s current pulse)

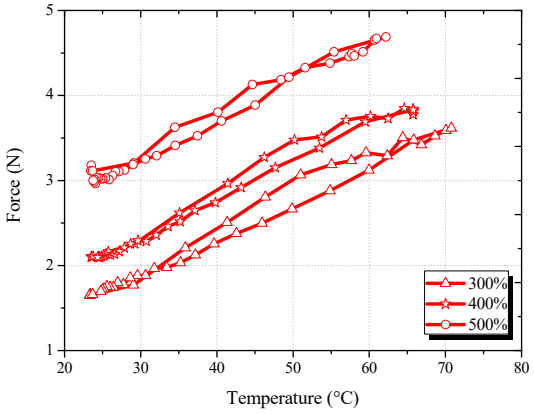

Fig.14: Hysteresis curves (15 s current pulse)

5. CONCLUSION

The electronic instrumentation developed to drive and measure the electrical, thermal and mechanical parameters of the shape memory alloy actuator was satisfactory; it was possible to determine the behavior of the SMA spring actuator on a test structure. According to the methodology used, the intended objectives were achieved, especially because the responses of force actuation in relation to time based on the chosen pulse widths, showing that the actuator can exert a force with the application of an electric current producing heat.

With respect to the parameters collected from the actuator, the hysteresis curves can be highlighted; these are important to define the operation of the actuator for a practical application, because they show force, temperature and heat loss simultaneously.

From the viewpoint of this project, with these curves it is possible to decide whether it is better to use an actuator with higher force capacity heated to higher temperature, with larger loss, or if it is better to decrease the parameter force, then the actuator has smaller losses. Even an intermediate situation can be chosen that meets best the actuator requirements.

ACKNOWLEDGMENT

The authors thank to the Active Structures and Systems Laboratory (LaSEA), Control and Instrumentation Laboratory (LINC), National Council for Scientific and Technological Development (CNPq) and the Coordination for the Improvement of Higher Level Education Personnel (Capes) for financing this research.

REFERENCES

Akash. K 1 , Mani P. S.S., Ashish K. S., Tameshwer N., Karthick S and Palani I. A. (2017), *Investigations on the Life cycle Behavior of Cu-Al-Ni/Polyimide Shape Memory Alloy Bi-morph at Varying Substrate Thickness and Actuation conditions*. vol. 254, pp. 28-35.

Basílio Sobrinho, J. M., Ferreira M. C., Souto, C. R., Silva, S. A., Santos, A. J. V. and Catunda, S. Y. C., (2017), *Electronic instrumentation for the characterization of a rotary thermoelectric motor driven by shape memory alloy springs*, IEEE International Instrumentation and Measurement Technology Conference (I2MTC) Turin, 2017 pp. 1-5. doi: 10.1109/I2MTC.2017.7969933.

Hau C. T., Gouwanda D., Gopalai A. A., Yee L. C. and Hanapiah F. A. (2017), *Design and Development of Platform Ankle Rehabilitation Robot with Shape Memory Alloy based Actuator*, pp. 946-948.

Hwang D. and Higuchi T. (2014), *A Rotary Actuator Using Shape Memory Alloy (SMA) Wires*, IEEE/ASME Transactions on Mechatronics, vol. 19.

Kim H., Han Y., Lee D., Ha J. and Cho K. (2012), *Sensorless displacement estimation of a shape memory alloy coil spring actuator using inductance,* Smart Materials and Structures, vol. 22.

Silva A. F. C., Santos A. J. V., Souto C. R., Araújo C. J., Silva S. A. (2013), *Artificial Biometric Finger Driven by Shape-MemoryAlloy Wires*, Artificial Organs, vol. 37, pp. 965–972.